

# Basic Nanoarchitectonics

Subjects: Nanoscience & Nanotechnology

Contributor: Katsuhiko Ariga

Although various synthetic methodologies including organic synthesis, polymer chemistry, and materials science are the main contributors to the production of functional materials, the importance of regulation of nanoscale structures for better performance has become clear with recent science and technology developments. Therefore, a new research paradigm to produce functional material systems from nanoscale units has to be created as an advancement of nanoscale science. This task is assigned to an emerging concept, nanoarchitectonics, which aims to produce functional materials and functional structures from nanoscale unit components. This can be done through combining nanotechnology with the other research fields such as organic chemistry, supramolecular chemistry, materials science, and bio-related science. In this review article, the basic-level of nanoarchitectonics is first presented with atom/molecular-level structure formations and conversions from molecular units to functional materials. Then, two typical application-oriented nanoarchitectonics efforts in energy-oriented applications and bio-related applications are discussed. Finally, future directions of the molecular and materials nanoarchitectonics concepts for advancement of functional nanomaterials are briefly discussed.

Keywords: bio-related application ; energy-oriented application ; nanoarchitectonics ; nanotechnology

---

## 1. Atom/Molecular-Level Nanoarchitectonics, Observation

The smallest level of nanoarchitectonics events occurs at the atom/molecular scales <sup>[1]</sup>. Molecular-scale events such as chemical reactions and molecular associations have been investigated traditionally by various spectral methods through collecting average information of numerous molecules in solution. However, rapid developments of probe microscopies and electron microscopes enable us to directly observe individual molecules and their behaviour. Atom/molecular-level nanoarchitectonics can be evaluated on the basis of direct observations.

Harano and co-authors have demonstrated various examples on observation of molecular behaviours with high spatial precisions and ultrashort resolutions using their technique, single-molecule atomic-resolution real-time electron microscopic (SMART-EM) with image recording <sup>[2][3]</sup>. For example, a single molecular level mechanical motions with sub-angstrom and sub-millisecond precision were recorded. Real-time recordings of nanoscale motions are realized using a fast camera with the aid of a denoising algorithm. Nanoarchitectonics design of entrapped fullerene molecules (C<sub>60</sub> molecules) within a carbon tube revealed shuttling and rotating behaviours of a single C<sub>60</sub> molecule (Figure 1) <sup>[4]</sup>. The molecular motions are coupled with carbon nanotube vibrations and can be observed in real-time mode with spatial resolution of 0.01 nm and standard error in time of 0.9 msec. The observed motions exhibited non-linear and stochastic natures and were often non-repeatable. This research revealed a molecular-level relationship between work and energy that had not been detected previously with time-averaged measurements and microscopic observations. In the used nanoarchitectonics motif, the carbon nanotube container and the entrapped C<sub>60</sub> molecules behaved together as a mechanical coupled oscillator to show characteristics of chaotic systems. These observations would explain the infrequent and stochastic motional behaviours of molecules attached to a carbon nanotube.

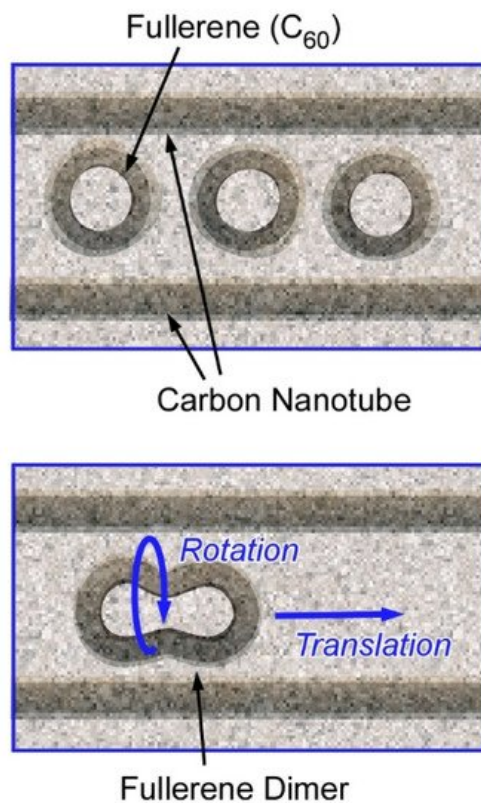


**Figure 1.** Nanoarchitectonics designs (models) of entrapment of fullerene molecules ( $C_{60}$  molecules) within a carbon tube for single-molecule atomic-resolution real-time electron microscopic (SMART-EM) with image recording.

Harano and co-workers also reported a single molecular level observation of molecular attachment to a surface of a carbon nanohorn (Figure 2) [5]. This chemical fishhook could capture a single molecule from its solution and transfer the captured molecule into the nm-scale view field of the electron microscope, which are essential processes in the SMART-EM technique. As the initial stem of the chemical fishhook, an aromatic group was installed on the surface of carbon nanohorns through the selective attachment reaction of in-situ-generated aryl radicals from arylamines to strained parts of the graphitic surface with negative and positive curvatures.

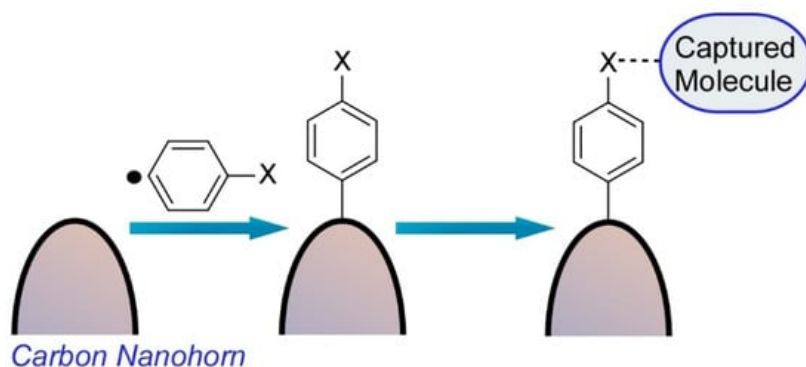


**Figure 2.** Molecular attachment to a surface of a carbon nanohorn for a single molecular level observation.

The other molecular moieties can be further attached through amide bond formation and/or be assembled upon van der Waals interaction from their solution. The aryl group was reacted perpendicular to the graphitic carbon nanohorn surface and otherwise physisorbed on the surface. Characteristics of a biradical resonance between two bowl-like strained pentagon moieties connected by aromatic linker were expected, but monoradical addition was only observed on the most strained apex of the carbon nanohorn. The second radical site may accept a hydrogen atom from the solvent used.

Fundamentals of coordination processes can be investigated with this technique. Atomic-level structure analyses on prenucleation clusters in syntheses of metal-organic frameworks (MOFs) were carried out using the SMART-EM technique by Harano and co-workers (Figure 3) [6]. As representative examples, two MOF structures (MOF-2 and MOF-5) can be obtained from the same precursors—zinc nitrate and benzene dicarboxylic acid—in dimethylformamide under different conditions.

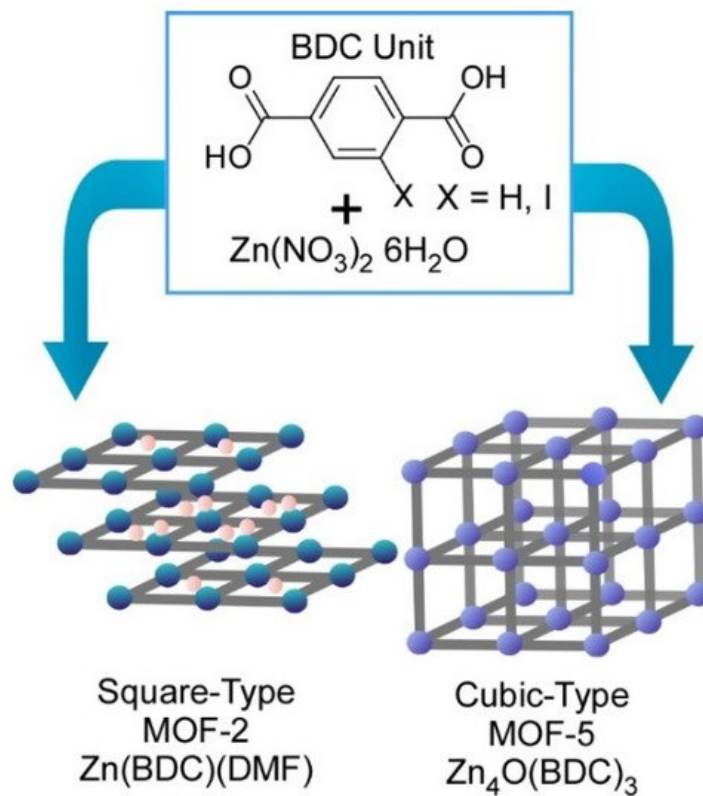


**Figure 3.** Two MOF structures (MOF-2 and MOF-5) obtained from the same precursors, zinc nitrate and benzene dicarboxylic acid in dimethylformamide under different conditions.

This research revealed processes to differentiate these two MOFs formation at resolution level at a single prenucleation cluster. Two different types of the prenucleation clusters were detected in the formation processes for MOF-2 and MOF-5 at 95 °C and 120 °C, respectively. Formation of a small amount of 1-nm-size cube and cube-like prenucleation clusters was identified during MOF-5 synthesis processes. These prenucleation clusters were in turn not detected in the MOF-2 formation process where linear and square prenucleation clusters were only found. Bifurcation between MOF-2 and MOF-5 was initiated even at the atomic structure level of prenucleation clusters. These basic structure features are nanoarchitected into crystal-level morphologies with square MOF-2 and the cubic MOF-5 lattices. Initiation of nanoarchitectonics process from metal ions and ligands to macroscopic MOF materials can be visualized by forefront microscopic techniques in the current technology.

## 2. Atom/Molecular-Level Nanoarchitectonics, Synthesis

Molecular level nanoarchitectonics are driven by non-covalent molecular associations and/or covalent organic reactions. Some innovative molecular-level nanoarchitectonics approaches from nanocarbon-related molecular nanoarchitectonics are exemplified below. As an example of the molecular association approach, Toyota et al. reported successful preparation of a nano-Saturn structure through supramolecular association between anthracene macrocyclic ring and ellipsoidal  $\text{C}_{70}$  molecule (Figure 4) [2]. Unlike typical supramolecular complex such as alkali ion trap by crown ethers, weaker CH- $\pi$  interactions have significant contributions in this ring-body supramolecular complex. Association constant of  $\text{C}_{70}$  molecules to the anthracene macrocyclic ring was twice larger than that for complex formation with  $\text{C}_{60}$  molecule. the central fullerene guest can float from the center of the ring without causing serious deterioration of their binding constant. This nanoarchitectonics motif is advantageous to form supramolecular complexes with non-spherical fullerenes.

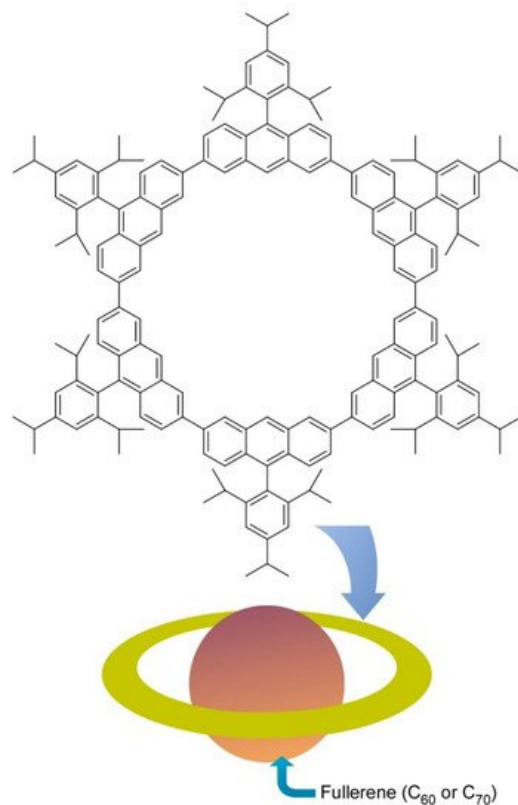


**Figure 4.** Nano-Saturn through supramolecular association between anthracene macrocyclic ring and ellipsoidal  $C_{70}$  molecule.

Several recent examples have demonstrated the contributions of skilled organic synthesis approaches to nanoarchitectonics to produce nanocarbon materials. Segawa and co-workers successfully demonstrated the synthesis of a carbon nanobelt, which is a closed loop of fully fused edge-sharing benzene rings (Figure 5A) [8]. The carbon nanobelt was synthesized through iterative Wittig reactions that were followed by a nickel-mediated aryl-aryl coupling reaction. It is expected to further nanoarchitect carbon nanotube materials with well-defined structures using the carbon nanobelt molecules as seed units. Carbon nanotube materials with uniform diameter and single chirality would be produced upon programmed synthesis with carbon nanobelt derivatives. Sun, and co-workers also demonstrated the synthesis of cylindrical  $C_{304}H_{264}$  molecules with 40 benzene (phenine) units bonded mutually at the 1, 3, and 5 positions as a finite phenine nanotube with periodic vacancy defects (Figure 5B) [9]. Nanoarchitecting carbon nanotubes with electronic properties modulatable by periodic vacancy defects upon fusion of the synthesized cylinder molecules were suggested by computational approaches.

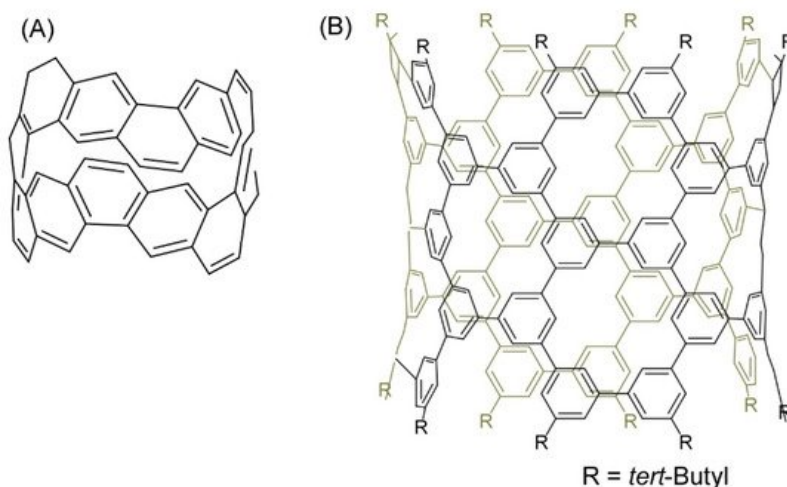


**Figure 5.** (A) Carbon nanobelt with a closed loop of fully fused edge-sharing benzene rings; (B) Cylindrical  $C_{304}H_{264}$  molecule with 40 benzene (phenine) units bonded mutually at the 1, 3, and 5 positions.

Nanoarchitectonics from organic molecules to two-dimensional nanocarbon has been also investigated as exemplified in a recent review article by Xu et al. [10][11][12]. Synthesis of the structure-defined graphene nanoribbons was accomplished through fusion of discrete polycyclic aromatic hydrocarbons at a solid surface. Therefore, this type of synthetic approach

is often called on-surface synthesis. [Figure 6](#) shows one example where precursor molecules with a dimethyltetracene core and two bromoanthryl units were fused into structure-defined graphene nanoribbons. Precisely prepared graphene nanostructures including graphene nanoribbons and graphene quantum dots are capable of having open bandgaps because of their quantum confinement effect. This characteristic is much different from zero-bandgap graphene and is attractive for semiconductor-related applications such as optoelectronics and nanoelectronics. However, preparation of precisely structurally controlled graphene nanostructures is difficult with conventional material processing. Bottom-up nanoarchitectonics from molecular precursors to well-defined nanocarbon with on surface synthesis would open many possibilities of nanocarbon technology.

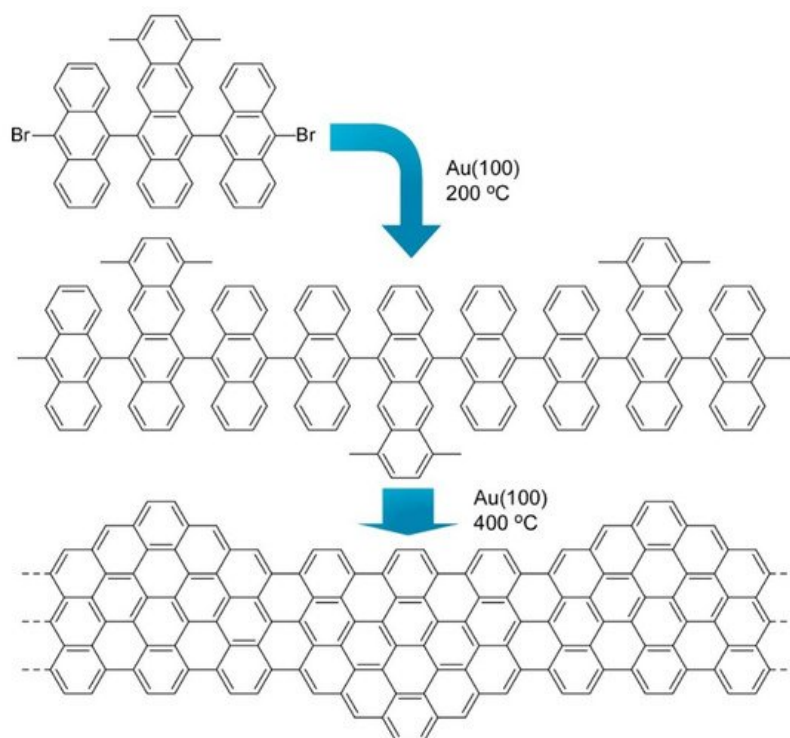


**Figure 6.** Fusion of molecules with a dimethyltetracene core and two bromoanthryl units into structure defined graphene nanoribbons.

Kawai and co-workers demonstrated on-surface synthesis for regioisomeric graphene nanoribbons through fusion of two kinds of precursor molecules ([Figure 7](#))<sup>[13]</sup>. Three different regioisomeric junctions were synthesized from 10,10'-dibromo-9,9'-bianthryl and 1,3,6,8-tetrabromopyrene on a Au (111) surface. When a sufficient amount of 10,10'-dibromo-9,9'-bianthryl relative to 1,3,6,8-tetrabromopyrene was supplied, 10,10'-dibromo-9,9'-bianthryl molecules were reacted at bromo-substituted sites in 1,3,6,8-tetrabromopyrene through an Ullmann-type reaction. Depending on the geometric relation between two reaction sites, subsequent cyclodehydrogenation upon high-temperature annealing resulted in graphene nanoribbon junctions with different connecting angles. Further analyses by scanning tunnelling spectroscopy with a CO-terminated tip with the aid of density functional theory (DFT) calculations revealed chemical structures and the electronic properties of these structure-defined graphene nanoribbons. The demonstrated nanoarchitectonics strategy would be applied to the other units to produce various carbon nanostructures. Nakamura et al. reported the synthesis of  $\pi$ -extended diaza[8]circulene through a combination of in-solution and on-surface syntheses ([Figure 8](#))<sup>[14]</sup>. The final form of  $\pi$ -extended diaza[8]circulene possessing six hexagons and two pentagons cannot be obtained only with solution-based reaction processes. The final cyclodehydrogenation step has to be done on a Au(111) surface.

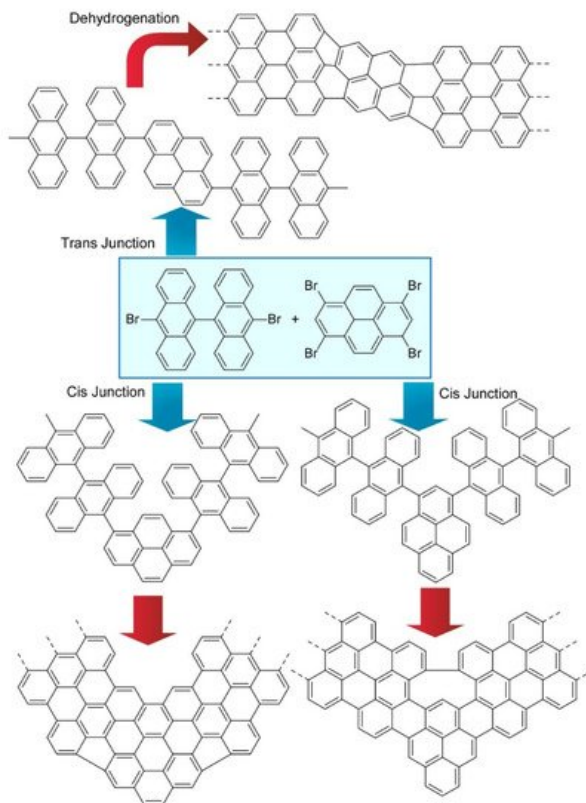


**Figure 7.** Three different regioisomeric junctions synthesized from 10,10'-dibromo-9,9'-bianthryl and 1,3,6,8-tetrabromopyrene on Au (111) surface.

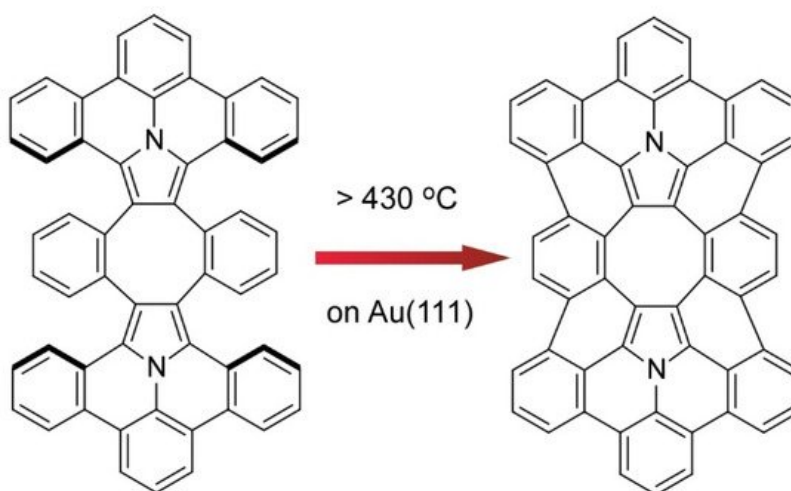


**Figure 8.** Synthesis of  $\pi$ -extended diaza[8]circulene through on-surface syntheses on a Au(111) surface.

In more advanced approaches to organic molecular nanoarchitectonics, tip-induced reactions have been investigated. Organic syntheses are mediated through molecular manipulations using the tip of probe microscopes that is called local probe chemistry. In a recent example reported by Kawai et al., three-dimensional graphene nanoribbons were first prepared by on-surface chemical reaction and tip-induced debromination with substitution reaction were demonstrated (Figure 9) [15]. The debromination process resulted in unstable radical species through cleaving the out-of-plane C-Br bond. The local probe chemistry was carried out at low temperature under ultra-high vacuum, which stabilized unstable debrominated radical species. Subsequently, a fullerene  $C_{60}$  molecule attached to the tip apex of the probe was directly transferred to the reactive radical site on graphene nanoribbon to complete substitution reactions. This example implies that nanoscale science would play important roles even in organic chemistry, which would enable us to synthesize target molecules through even atom-by-atom nanoarchitectonics.

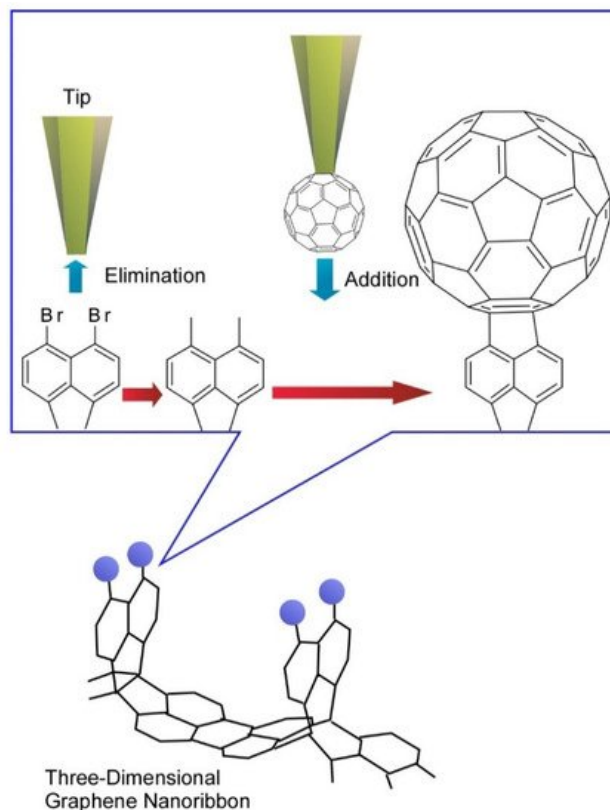


**Figure 9.** Tip-induced debromination with substitution reaction with fullerene molecule were at three-dimensional graphene nanoribbon.

Tip-mediated manipulations can be applicable to inorganic semiconductor materials as reported by Hasegawa and co-workers who proposed a nanoarchitectonics strategy to control the numbers of dopant atoms within solid electrolyte nanostructures (Figure 10) [16]. A Pt tip was positioned above  $\alpha\text{-Ag}_{2+\delta}\text{S}$  nanodots as a model system with non-stoichiometry excess dopants at a tunnelling distance. Electrochemical precipitation of Ag atoms to form a Ag protrusion was initiated when the bias voltage was increased to 100 mV. Step heights of protrusion growth corresponded to multiples of single atomic plane of Ag (111) and finally reached to equilibrated height at the given bias. These stepwise precipitations of Ag resulted in tuning of the numbers of excess dopants at an atomic level. As the results, atom-by-atom-level tuning of electrochemical potential energy can be achieved. The proposed nanoarchitectonics approach to manipulate the numbers of dopant atoms in solid electrolyte materials upon control of applied bias leads to discrete regulation of electrical properties of nanomaterials. Eventually, this could become a promising method to develop nanomaterial devices with single ion/atom transfer capability.

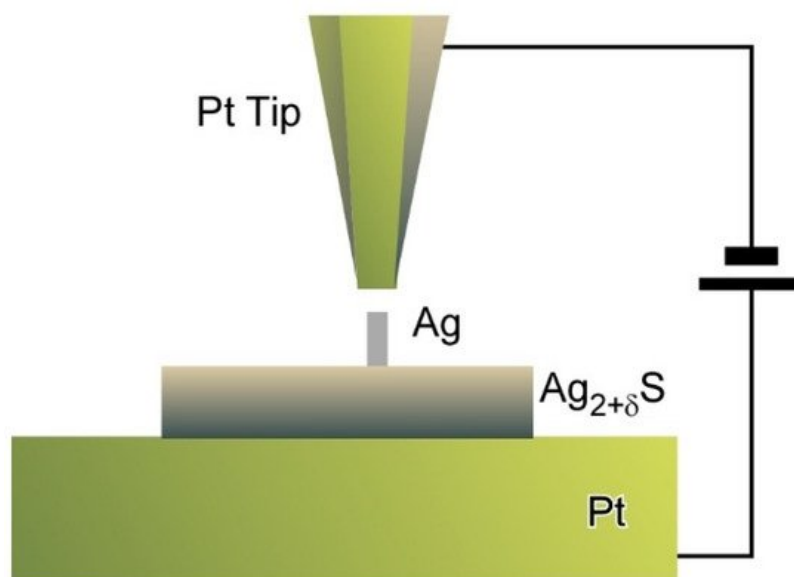


**Figure 10.** Nanoarchitectonics strategy to control the numbers of dopant atoms within solid electrolyte nanostructures using a Pt tip.

Another target of atomic-level precise nanoarchitectonics would be synthesis of metal clusters with discrete numbers of atoms. Ultimately, functional metal clusters are desirably prepared in ultraprecise control of their size at a single atom level. In a recent review article by Imaoka and Yamamoto [17][18][19], chemical approaches to synthesize atomically precise metal clusters are discussed. Their strategies basically utilized basicity gradient within structurally defined dendrimers to which metal ions can be coordinated. In the case of the dendrimer template depicted in Figure 11, 12 metal ions can be coordinated at the coordination sites up to the dendrimer second layer and 28 atoms can coordinate up to the third layer. Based on the clear differences of the basicity of coordination sites between the second and third layers, discrete numbers of metal ions were isolated within the dendrimer cores to give metal cluster with precisely controlled number (12 atoms). For example, synthesis with use of phenylazomethine-based dendrimer template provided atomically controlled Pt clusters on the basis of sufficient basicity gradient strength of the dendrimer template.

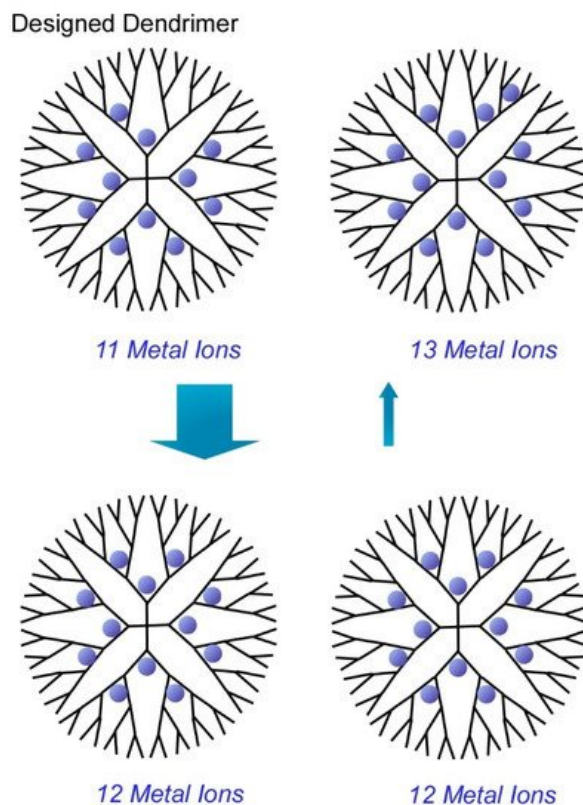


**Figure 11.** Structurally defined dendrimer cores to give metal cluster with precisely controlled number (12 atoms).

These examples demonstrate various types of atom/molecular-level nanoarchitectonics to create functional structures and materials from atomic and molecular structural units. In addition to chemical techniques and surface sciences, nanotechnological tools such as tips of probe microscopies are used in advanced examples. Although organic syntheses are recognized as well-established research fields, advanced nanoscale technique can open new pages even in this classic science. This would be a successful nanoarchitectonics example of field fusion between nanotechnology and traditional science.

### 3. Nanoarchitectonics toward Materials

In order to prepare functional systems useful in many occasions, conversion from molecular units (or nanomaterial units) to functional materials is a crucial process. In such conversions, reflection of structural and functional features of nanounits is important to keep the high functions in material level. These nanoarchitectonics processes from nano to materials have potential contributions to many research fields including supramolecular chemistry [20][21][22][23] and materials chemistry [24][25][26][27] although they were not recognized as parts of nanoarchitectonics. However, many of them bear features of material-level nanoarchitectonics. For preparation for nanofeature-bearing functional materials, various assistant factors such as guiding by template structures and asymmetrical structure formation at interfacial environments have important roles in addition to conventional self-assembly.

For example, Kawai and co-workers successfully synthesized ultrathin Au nanowires in aqueous systems with guiding of molecular assemblies of ascorbic acid derivatives, and subsequent alignment of the synthesized Au nanowires with precise intervals was demonstrated (Figure 12) [28]. Au nanowires with a diameter of ca. 1.7 nm were fabricated through an oriented attachment growth mechanism. Ascorbic acid derivatives with octadecyl chains weakly attached on the Au(111) crystal face induced oriented growth of the Au nanowire. Elongation of the nanowires was effectively facilitated in

the presence of  $\text{Cl}^-$  ions to give nanowires with a length of over a few  $\mu\text{m}$ . Drying processes of the aqueous Au nanowire solutions on a solid substrate resulted in parallel allays of the Au nanowires with regular wire-by-wire intervals. Mainly narrow intervals of 2.9 nm and wide intervals of 9.1 nm were observed. The former intervals (2.9 nm) correspond to the thickness of the interdigitated bilayer of the ascorbic acid derivatives. Formation of a non-interdigitated four layer (double bilayer) between the Au nanowires can explain the wide interval (9.1 nm). These examples demonstrate that simple amphiphile assemblies can guide the formation of micro-level structures with sub-nanometer-level internal structural precision.

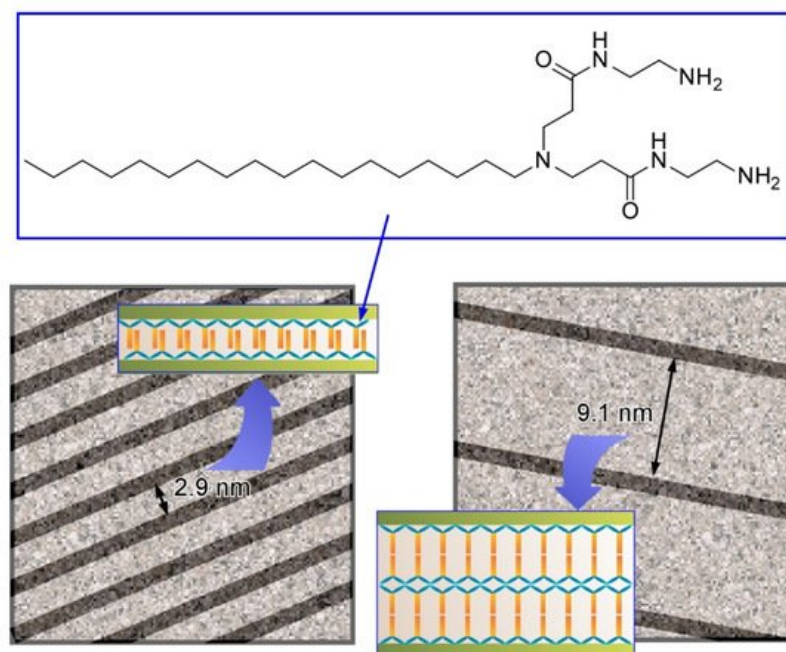


**Figure 12.** Parallel allays of the Au nanowires with regular wire-by-wire intervals (models) with narrow interval of 2.9 nm and wide interval of 9.1 nm, corresponding to interdigitated bilayer and non-interdigitated four layer of the ascorbic acid derivatives, respectively.

A similar guiding method can be applied to other material systems. As summarized an extensive recent review article by Akagi [29][30], chiral conjugate polymer materials with the guide of chiral liquid crystalline templates. Helical screw directions (materials chirality) can be selected by the chiral dopants in liquid crystals. Controlled helical structures of conjugated polymers was led to chiroptical properties such as circularly polarized luminescence. Furthermore, helical conjugate polymer materials can be converted into graphitic carbons without causing structural deteriorations of the original helical structures by iodine-doped carbonization.

Interfaces are nice playgrounds to produce various functional material properties [31]. Nanoarchitectonics at interfaces is advantageous for delicate tuning of functions [32]. For example, Ajayaghosh and co-workers delicately nanoarchitected the surface of conventional alumina materials to regenerate the bio-like wettability functions of rose petal and lotus leaf effects (Figure 13) [33]. The former effect induces sticky water droplets through droplets pinned on surface nanostructures, and slippery water droplets are observed with the latter effect with droplet sitting on the top surface of the nanostructures. Intrinsically hydrophilic aluminum surface was first modified with (*E*)-4,4'-(diazene-1,2-diyl)bis(4,1-phenylene))bis(oxy)dibutanoic acid to give a water contact angle of  $145^\circ$  with high contact angle hysteresis of  $\pm 69^\circ$  advantageous for water sticking. Further coordination with  $\text{Zn}^{2+}$  ions resulted in a higher contact angle to water ( $165^\circ$ ) and lower contact angle hysteresis ( $\pm 2^\circ$ ) for water slipping. In both the cases, coating with an aromatic bis-aldehyde with alkoxy chain substituents were required to express rose petal and lotus leaf effects. This adduct worked as nanowaxy cuticle in naturally occurring systems. Surface nanoarchitectonics with light tuning of modification and coating structures can convert conventional alumina materials into bio-like functional surfaces.

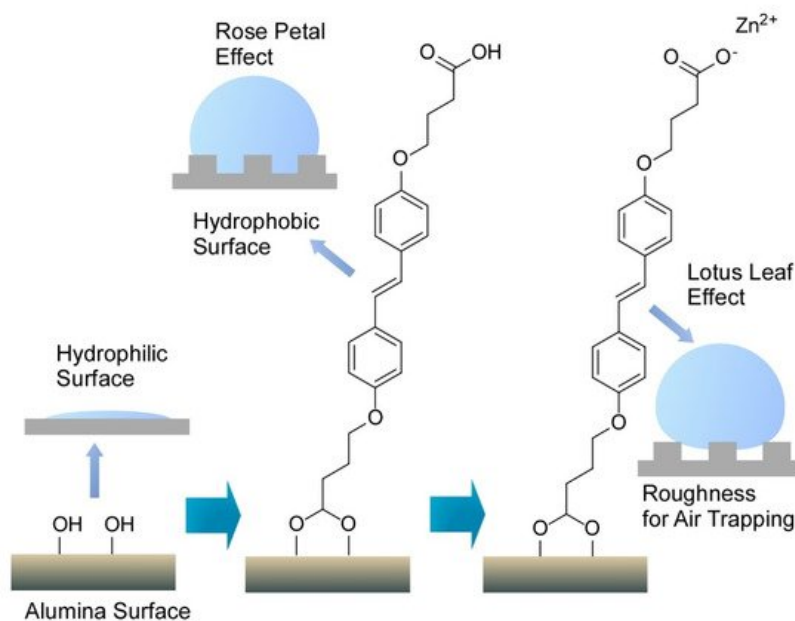


**Figure 13.** Surface nanoarchitectonics of conventional alumina materials to regenerate bio-like wettability functions of rose petal and lotus leaf effects where single molecule in assembled structure is only depicted.

Liquid surfaces such as gas-liquid interfaces and liquid-liquid interfaces have several advantages for nanoarchitectonics processes from molecular/nanomaterial level to functional materials. Interfacial environments between two immiscible liquids would give encountering opportunities for molecular components with different solvent affinities. These situations are well suited to nanoarchitect two-dimensional metal-organic frameworks (MOFs) [34][35][36] and covalent organic frameworks (COFs) [37][38][39]. Drastic changes of component solubilities at liquid-liquid interfaces are used for materials nanoarchitectonics through liquid-liquid interfacial precipitation. For example, upon the liquid-liquid interfacial precipitation, fullerene molecules ( $C_{60}$ ,  $C_{70}$  and so on) can be nanoarchitectured into various nano and microstructures [40][41][42] including one-dimensional rods/tubes/whiskers [43][44], two-dimensional sheets [45][46], three-dimensional cubes [47], hierarchical structures such as rod-on-cube [48][49] and hole-in-cube [50], and the other integrated structures [51][52][53].

## 4. Langmuir-Blodgett Nanoarchitectonics

As one of the typical thin film nanoarchitectonics methods, the Langmuir-Blodgett (LB) technique [54][55][56][57] is basically used at the air-water interface, where molecular recognition capabilities are drastically enhanced as compared with bulk aqueous phase [56][57], which has been demonstrated experimentally [58][59][60][61], spectroscopically [62][63][64][65], and theoretically [66][67]. This nature can be used for preparation of two-dimensional molecular patterns which have macroscopic lateral dimensions and sub-nanometer-level internal pattern structures [68]. Highly anisotropic motional freedoms at the air-water interface enable us to manipulate molecules by macroscopic motion like hand motion [69][70]. Macroscopic motions such as sub-meter-level compression and expansion of Langmuir monolayer in lateral direction can be coupled with molecular-level functions within nanometer-level thickness at the air-water interface. Regulation of molecular machines [71] by hand-like macroscopic mechanical motions such as reversible guest capture [72][73], enantioselective amino acid discrimination [74], faint tuning of nucleic acid base recognition [75], control of fluorescence resonance energy transfer [76], molecular rotor rotation [77][78], molecular pliers operation [79][80], molecular flapping [81], and nanocar actions [82] have been actually demonstrated. As depicted in Figure 14, faint orientational changes of double-paddled binuclear  $Pt^{II}$  complexes through macroscopic mechanical compression of their monolayer at the air-water interface [83]. Molecular-level orientation change of the binuclear  $Pt^{II}$  complexes into chromophore emergence from water through molecular flapping from perpendicular to parallel was successfully induced accompanied with a drastic increase of phosphorescence. This emission increase by floating-up molecules from aqueous phase is called submarine emission.

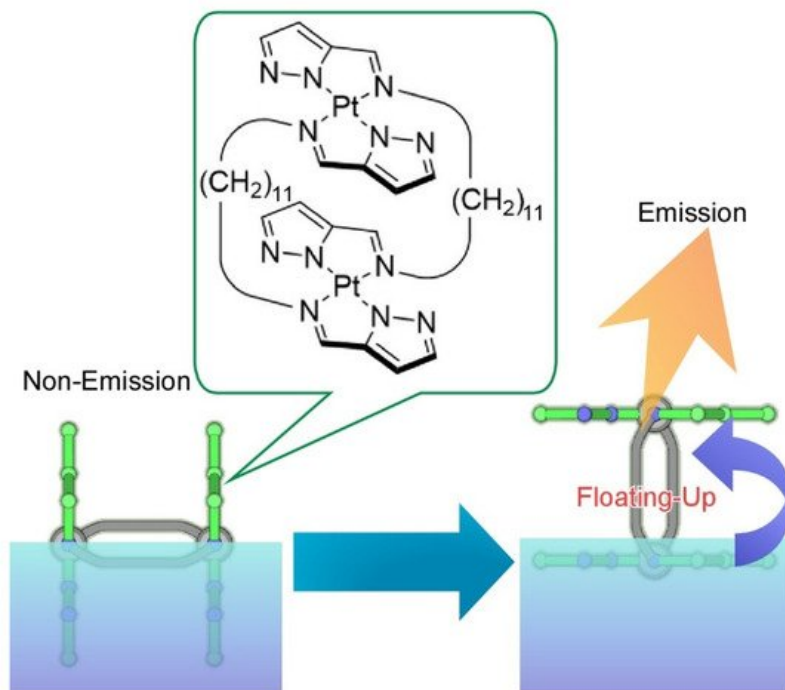


**Figure 14.** Faint orientational changes of double-paddled binuclear Pt<sup>II</sup> at the air-water interface from perpendicular to parallel accompanied with drastic increase of phosphorescence, as called submarine emission.

With dynamic process at the air-water interface, molecular precursors can be converted into structure-controlled nanomaterials as exemplified in [Figure 15](#) <sup>[84]</sup>. In this case, carbon ring molecule (9,9',10,10'-tetrabutoxycyclo-[6]-paraphenylene-[2]-3,6-phenanthrenylene) was selected as a molecular precursor. A molecular film of the carbon ring molecule was first spread through dropping its chloroform solution onto a water with a vortex rotating motion. This is called the vortex Langmuir-Blodgett (vortex LB) method <sup>[85]</sup>. Two-dimensional uniform thin films of carbon ring molecules were formed with the aid of vortex motion of the water phase. Analyses on the transferred film from the water surface onto a solid substrate revealed a uniform ultrathin nature (thickness of ca. 10 nm and width of tens of micrometers) and insulative properties. Calcination of the transferred film at 850 °C for 3 h under a N<sub>2</sub> gas flow successfully converted the assembled film from a nanocarbon film without any structural deterioration accompanied with drastic increase of electrical conductivity ( $1.98 \times 10^3 \text{ Sm}^{-1}$ ). Addition of pyridine during the initial vortex LB process efficiently resulted in nitrogen-doped carbon nanosheets with further increase of conductivity. Easy nanoarchitectonics methods from simple molecules into nitrogen-doped carbon nanosheet would become useful for preparation of efficient catalysts for oxygen reduction reactions in fuel cell applications.

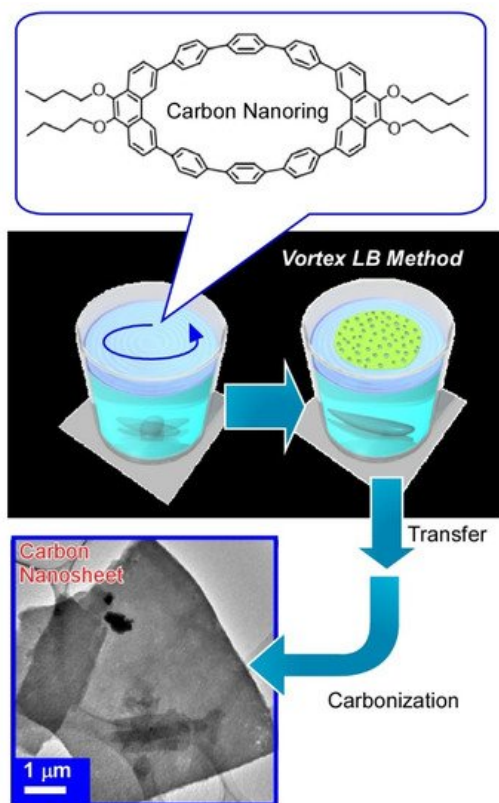


**Figure 15.** Nanoarchitectonics for preparation of carbon nanosheet from carbon ring molecule (9,9',10,10'-tetrabutoxy-cyclo-[6]-paraphenylene-[2]-3,6-phenanthrylene) through vortex Langmuir-Blodgett (vortex LB) method and calcination at 850 °C under N<sub>2</sub> gas flow.

In nanoarchitectonics processes from molecules to materials, regulation of molecular orientations within the nanoarchitectured materials becomes key one of the important key factor for functions. As described in a recent review article by Kido and co-workers [96][97][98], molecular orientation is an indispensable factor to achieve high performances in organic light-emitting devices. They even expect that molecular engineering to nanoarchitect horizontal molecular orientation would open a golden era of vibrant research for organic light-emitting devices. Therefore, nanoarchitectonics methods to achieve well-controlled molecular orientation in materials such as ultrathin films become crucially important. Some established techniques such as the LB method [89][90] and layer-by-layer (LbL) assembly [91][92][93] have been applied to this task. However, fabrication of functional molecules and polymers into well-organized high quality thin films is not always easy, unlike conventional assembly of lipid molecules. Functional molecules with conjugated aromatic cores tend to form undesirable aggregates even in these conventional fabrication processes for ultrathin films.

Very recently, Ito et al. have demonstrated a breakthrough method, the 100 °C-Langmuir-Blodgett (100-LB) method, to fabricate highly oriented uniform ultrathin films of polymeric semiconductors (Figure 16) [94]. In common sense of science and technology, a conventional LB method is conducted at around room temperature. Because of unavoidable disturbances by vapours of water as a subphase liquid, LB processes above 40 °C are usually unfavourable. This limitation of operational temperature ranges is not advantageous to suppress undesirable aggregations of aromatic conjugate molecules. Ito et al. used ethylene glycol as a solvent for the subphase instead of water. The liquid range of ethylene glycol (−12.9 to 197.3 °C) led to a wide operational temperature for the LB technique where relatively low vapor pressures and high surface tensions can be maintained. Actually, LB film preparation was demonstrated up to 100 °C using a polymeric semiconductor molecule, poly[2,5-bis(3-tetradecylthiophen-2-yl)thieno(3,2-b)-thiophene] (PBTTT), which is known as a highly aggregative polymers with low solubility.

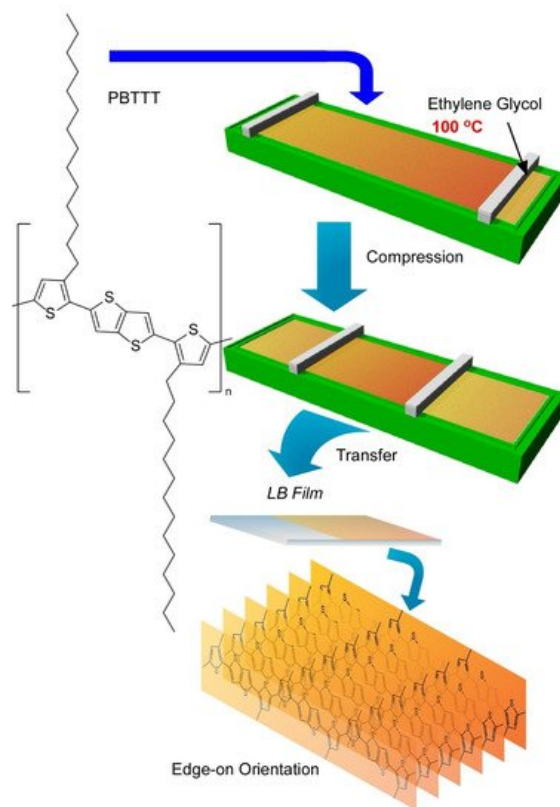


**Figure 16.** A novel method, 100 °C-Langmuir-Blodgett (100-LB) technique to fabricate highly oriented uniform ultrathin films with edge-on orientation of polymeric semiconductors, poly[2,5-bis(3-tetradecylthiophen-2-yl)thieno(3,2-b)-thiophene] (PBTTT), on ethylene glycol as a solvent for subphase.

Thin films of this polymeric semiconductors were prepared through Langmuir-Schaefer-type transfer of surface films that were compressed after spreading at various temperatures up to 100 °C. LB films with defined thickness with high homogeneity over millimeter scales were obtained. Observation of the film surface morphology by laser confocal microscopy verified this high film homogeneity. High contrast in polarized optical microscopy images with different polarization angle implied significant orientation of the film where the main chains of polymeric semiconductor was highly oriented at least in a length scale of several hundred micrometer. Further analyses of the LB films with grazing incidence X-ray diffractions and grazing incidence wide-angle X-ray scattering revealed uniaxially aligned highly crystalline nature with edge-on lamellar orientation that is desirable for facilitated charge transport. The degree of crystallinity and alignment the LB films of the polymeric semiconductor tended to be enhanced with the increase of process temperature. The mobilities along the direction parallel to main polymer chains for the LB films prepared at 80 °C were obtained as high as  $0.54 \text{ cm}^2\text{V}^{-1}\text{s}^{-1}$ . The obtained values are much higher than those observed for conventional thin films and that for room-temperature prepared LB film ( $0.17 \text{ cm}^2\text{V}^{-1}\text{s}^{-1}$ ). The mobility parallel to main chains of the polymeric semiconductor in LB films prepared at 80 °C was eight times higher than that measured for the perpendicular direction to the main chains in the same LB film. These facts clearly proves the excellent performances of the polymeric semiconductor films based on higher degree of crystallinity and unidirectional properties through nanoarchitectonics of the high temperature LB technique.

As mentioned above, nanoarchitectonics from molecules to materials can produce various possibilities of functional materials with inside nano-organized structure. Interfacial processes that often play important roles in the fabrication of materials with nanostructure-based functions <sup>[95][96]</sup>.

## References

1. Ariga, K. Atomic and organic nanoarchitectonics. *Trends Chem.* 2020, 2, 779–782.
2. Nakamura, E. Atomic-resolution transmission electron microscopic movies for study of organic molecules, assemblies, and reactions: The first 10 years of development. *Acc. Chem. Res.* 2017, 50, 1281–1292.
3. Harano, K. Self-assembly mechanism in nucleation processes of molecular crystalline materials. *Bull. Chem. Soc. Jpn.* 2021, 94, 463–472.
4. Shimizu, T.; Lungerich, D.; Stuckner, J.; Murayama, M.; Harano, K.; Nakamura, E. Real-time video imaging of mechanical motions of a single molecular shuttle with sub-millisecond sub-angstrom precision. *Bull. Chem. Soc. Jpn.*

5. Kamei, K.; Shimizu, T.; Harano, K.; Nakamura, E. Aryl radical addition to curvatures of carbon nanohorns for single-molecule-level molecular imaging. *Bull. Chem. Soc. Jpn.* 2020, 93, 1603–1608.
6. Xing, J.; Schweighauser, L.; Okada, S.; Harano, K.; Nakamura, E. Atomistic structures and dynamics of prenucleation clusters in MOF-2 and MOF-5 syntheses. *Nat. Commun.* 2019, 10, 3608.
7. Toyota, S.; Yamamoto, Y.; Wakamatsu, K.; Tsurumaki, E.; Muñoz-Castro, A. Nano-Saturn with an ellipsoidal body: Anthracene macrocyclic ring-C70 complex. *Bull. Chem. Soc. Jpn.* 2019, 92, 1721–1728.
8. Povie, G.; Segawa, Y.; Nishihara, T.; Miyauchi, Y.; Itami, K. Synthesis of a carbon nanobelt. *Science* 2017, 356, 172–175.
9. Sun, Z.; Ikemoto, K.; Fukunaga, T.M.; Koretsune, T.; Arita, R.; Sato, S.; Isobe, H. Finite phenine nanotubes with periodic vacancy defects. *Science* 2019, 363, 151–155.
10. Xu, X.; Müllen, K.; Narita, A. Syntheses and characterizations of functional polycyclic aromatic hydrocarbons and graphene nanoribbons. *Bull. Chem. Soc. Jpn.* 2020, 93, 490–506.
11. Müllen, K. Evolution of graphene molecules: Structural and functional complexity as driving forces behind nanoscience. *ACS Nano* 2014, 8, 6531–6541.
12. Gröning, O.; Wang, S.; Yao, X.; Pignedoli, C.A.; Borin, G.; Daniels, B.C.; Cupo, A.; Meunier, V.; Feng, X.; Narita, A.; et al. Engineering of robust topological quantum phases in graphene nanoribbons. *Nature* 2018, 560, 209–213.
13. Sun, K.; Krejčí, O.; Foster, A.S.; Okuda, Y.; Orita, A.; Kawai, S. Synthesis of regioisomeric graphene nanoribbon junctions via heteroprecursors. *J. Phys. Chem. C* 2019, 123, 17632–17638.
14. Nakamura, K.; Li, Q.-Q.; Krejčí, O.; Foster, A.S.; Sun, K.; Kawai, S.; Ito, S. On-surface synthesis of a  $\pi$ -extended diaza[8]circulene. *J. Am. Chem. Soc.* 2020, 142, 11363–11369.
15. Kawai, S.; Krejčí, O.; Nishiuchi, T.; Sahara, K.; Kodama, T.; Pawlak, R.; Meyer, E.; Kubo, T.; Foster, A.S. Three-dimensional graphene nanoribbons as a framework for molecular assembly and local probe chemistry. *Sci. Adv.* 2020, 6, eaay8913.
16. Nayak, A.; Unayama, S.; Tai, S.; Tsuruoka, T.; Waser, R.; Aono, M.; Valov, I.; Hasegawa, T. Nanoarchitectonics for controlling the number of dopant atoms in solid electrolyte nanodots. *Adv. Mater.* 2018, 30, 1703261.
17. Imaoka, T.; Yamamoto, K. Wet-chemical strategy for atom-precise metal cluster catalysts. *Bull. Chem. Soc. Jpn.* 2019, 92, 941–948.
18. Yamamoto, K.; Higuchi, M.; Shiki, S.; Tsuruta, M.; Chiba, H. Stepwise radial complexation of imine groups in phenylazomethine dendrimers. *Nature* 2002, 415, 509–511.
19. Yamamoto, K.; Imaoka, T. Dendrimer Complexes Based on Fine-Controlled Metal Assembling. *Bull. Chem. Soc. Jpn.* 2006, 79, 511.
20. Cortez, M.L.; Lorenzo, A.; Marmisollé, W.A.; Von Bilderling, C.; Maza, E.; Pietrasanta, L.I.; Battaglini, F.; Ceolín, M.; Azzaroni, O. Azzaroni, Highly-organized stacked multilayers via layer-by-layer assembly of lipid-like surfactants and polyelectrolytes. Stratified supramolecular structures for (bio)electrochemical nanoarchitectonics. *Soft Matter* 2018, 14, 1939–1952.
21. Ariga, K.; Shrestha, L.K. Supramolecular nanoarchitectonics for functional materials. *APL Mater.* 2019, 7, 120903.
22. Sang, Y.; Liu, M. Nanoarchitectonics through supramolecular gelation: Formation and switching of diverse nanostructures. *Mol. Syst. Des. Eng.* 2019, 4, 11–28.
23. Ariga, K.; Mori, T.; Kitao, T.; Uemura, T. Supramolecular chiral nanoarchitectonics. *Adv. Mater.* 2020, 32, 1905657.
24. Komiyama, M.; Mori, T.; Ariga, K. Molecular imprinting: Materials nanoarchitectonics with molecular information. *Bull. Chem. Soc. Jpn.* 2018, 91, 1075–1111.
25. Sangian, D.; Ide, Y.; Bando, Y.; Rowan, A.E.; Yamauchi, Y. Materials nanoarchitectonics using 2D layered materials: Recent developments in the intercalation process. *Small* 2018, 14, 1800551.
26. Azhar, A.; Li, Y.; Cai, Z.; Zakaria, M.B.; Masud, M.K.; Hossain, M.S.A.; Kim, J.; Zhang, W.; Na, J.; Yamauchi, Y.; et al. Nanoarchitectonics: A new materials horizon for Prussian blue and its analogues. *Bull. Chem. Soc. Jpn.* 2019, 92, 875–904.
27. Ariga, K.; Jia, X.; Shrestha, L.K. Soft material nanoarchitectonics at interfaces: Molecular assembly, nanomaterial synthesis, and life control. *Mol. Syst. Des. Eng.* 2019, 4, 49–64.
28. Miyajima, N.; Wang, Y.-C.; Nakagawa, M.; Kurata, H.; Imura, Y.; Wang, K.-H.; Kawai, T. Water-phase synthesis of ultrathin Au nanowires with a two-dimensional parallel array structure. *Bull. Chem. Soc. Jpn.* 2020, 93, 1372–1377.

29. Akagi, K. Interdisciplinary chemistry based on integration of liquid crystals and conjugated polymers: Development and progress. *Bull. Chem. Soc. Jpn.* 2019, 92, 1509–1655.
30. Akagi, K.; Piao, G.; Kaneko, S.; Sakamaki, K.; Shirakawa, H.; Kyotani, M. Helical polyacetylene synthesized with a chiral nematic reaction field. *Science* 1998, 282, 1683–1686.
31. Ariga, K.; Ishii, M.; Mori, T. 2D nanoarchitectonics: Soft interfacial media as playgrounds for microobjects, molecular machines, and living cells. *Chem. Eur. J.* 2020, 26, 6461–6472.
32. Ariga, K. Molecular tuning nanoarchitectonics for molecular recognition and molecular manipulation. *ChemNanoMat* 2020, 6, 870–880.
33. Mukhopadhyay, R.D.; Vedhanarayanan, B.; Ajayaghosh, A. Creation of “rose petal” and “lotus leaf” effects on alumina by surface functionalization and metal-ion coordination. *Angew. Chem. Int. Ed.* 2017, 56, 16018–16022.
34. Makiura, R.; Motoyama, S.; Umemura, Y.; Yamanaka, H.; Sakata, O.; Kitagawa, H. Surface nano-architecture of a metal-organic framework. *Nat. Mater.* 2020, 9, 565–571.
35. Sakamoto, R.; Takada, K.; Sun, X.; Pal, T.; Tsukamoto, T.; Phua, E.J.H.; Rapakousiou, A.; Hoshiko, K.; Nishihara, H. The coordination nanosheet (CONASH). *Coord. Chem. Rev.* 2016, 320, 118–128.
36. Duan, J.; Li, Y.; Pan, Y.; Behera, N.; Jin, W. Metal-organic framework nanosheets: An emerging family of multifunctional 2D materials. *Coord. Chem. Rev.* 2019, 395, 25–45.
37. Côté, A.P.; Benin, A.I.; Ockwig, N.W.; O’Keeffe, M.; Matzger, A.J.; Yaghi, O.M. Porous, crystalline, covalent organic frameworks. *Science* 2005, 310, 1166–1170.
38. Ariga, K.; Matsumoto, M.; Mori, T.; Shrestha, L.K. Materials nanoarchitectonics at two-dimensional liquid interfaces. *Beilstein J. Nanotechnol.* 2019, 10, 1559–1587.
39. Geng, K.; He, T.; Liu, R.; Dalapati, S.; Tan, K.T.; Li, Z.; Tao, S.; Gong, Y.; Jiang, Q.; Jiang, D. Covalent organic frameworks: Design, synthesis, and functions. *Chem. Rev.* 2020, 120, 8814–8933.
40. Shrestha, L.K.; Ji, Q.; Mori, T.; Miyazawa, K.; Yamauchi, Y.; Hill, J.P.; Ariga, K. Fullerene nanoarchitectonics: From zero to higher dimensions. *Chem. Asian J.* 2013, 8, 1662–1679.
41. Ariga, K.; Shrestha, L.K. Fullerene nanoarchitectonics with shape-shifting. *Materials* 2020, 13, 2280.
42. Ariga, K.; Shrestha, L.K. Zero-to-one (or more) nanoarchitectonics: How to produce functional materials from zero-dimensional single-element unit, fullerene. *Mater. Adv.* 2021, 2, 582–597.
43. Shrestha, L.K.; Shrestha, R.G.; Yamauchi, Y.; Hill, J.P.; Nishimura, T.; Miyazawa, K.; Kawai, T.; Okada, S.; Wakabayashi, K.; Ariga, K. Nanoporous carbon tubes from fullerene crystals as the  $\pi$ -electron carbon source. *Angew. Chem. Int. Ed.* 2015, 54, 951–955.
44. Minami, K.; Kasuya, Y.; Yamazaki, T.; Ji, Q.; Nakanishi, W.; Hill, J.P.; Sakai, H.; Ariga, K. Highly ordered 1D fullerene crystals for concurrent control of macroscopic cellular orientation and differentiation toward large-scale tissue engineering. *Adv. Mater.* 2015, 27, 4020–4026.
45. Sathish, M.; Miyazawa, K.; Hill, J.P.; Ariga, K. Solvent engineering for shape-shifter pure fullerene (C60). *J. Am. Chem. Soc.* 2009, 131, 6372–6373.
46. Shrestha, L.K.; Yamauchi, Y.; Hill, J.P.; Miyazawa, K.I.; Ariga, K. Fullerene Crystals with Bimodal Pore Architectures Consisting of Macropores and Mesopores. *J. Am. Chem. Soc.* 2013, 135, 586–589.
47. Bairi, P.; Tsuruoka, T.; Acharya, S.; Ji, Q.; Hill, J.P.; Ariga, K.; Yamauchi, Y.; Shrestha, L.K. Mesoporous fullerene C70 cubes with highly crystalline frameworks and unusually enhanced photoluminescence properties. *Mater. Horiz.* 2018, 5, 285–290.
48. Shrestha, L.K.; Sathish, M.; Hill, J.P.; Miyazawa, K.; Tsuruoka, T.; Sanchez-Ballester, N.M.; Honma, I.; Ji, Q.; Ariga, K. Alcohol-induced decomposition of Olmstead’s crystalline Ag(I)–fullerene heteronanostructure yields ‘bucky cubes’. *J. Mater. Chem. C* 2013, 1, 1174–1181.
49. Bairi, P.; Minami, K.; Nakanishi, W.; Hill, J.P.; Ariga, K.; Shrestha, L.K. Hierarchically structured fullerene C70 cube for sensing volatile aromatic solvent vapors. *ACS Nano* 2016, 10, 6631–6637.
50. Bairi, P.; Minami, K.; Hill, J.P.; Ariga, K.; Shrestha, L.K. Intentional closing/opening of “hole-in-cube” fullerene crystals with microscopic recognition properties. *ACS Nano* 2017, 11, 7790–7796.
51. Bairi, P.; Minami, K.; Hill, J.P.; Nakanishi, W.; Shrestha, L.K.; Liu, C.; Harano, K.; Nakamura, E.; Ariga, K. Supramolecular differentiation for construction of anisotropic fullerene nanostructures by time-programmed control of interfacial growth. *ACS Nano* 2016, 10, 8796–8802.

52. Tang, Q.; Maji, S.; Jiang, B.; Sun, J.; Zhao, W.; Hill, J.P.; Ariga, K.; Fuchs, H.; Ji, Q.; Shrestha, L.K. Manipulating the structural transformation of fullerene microtubes to fullerene microhorns having microscopic recognition properties. *ACS Nano* 2019, 13, 14005–14012.
53. Hsieh, C.-T.; Hsu, S.-h.; Maji, S.; Chahal, M.K.; Song, J.; Hill, J.P.; Ariga, K.; Shrestha, L.K. Post-assembly dimension-dependent face-selective etching of fullerene crystals. *Mater. Horiz.* 2020, 7, 787–795.
54. Ariga, K.; Mori, T.; Li, J. Langmuir nanoarchitectonics from basic to frontier. *Langmuir* 2019, 35, 3585–3599.
55. Sato, H.; Takimoto, K.; Kato, M.; Nagaoka, S.; Tamura, K.; Yamagishi, A. Real-time monitoring of low pressure oxygen molecules over wide temperature range: Feasibility of ultrathin hybrid films of iridium(III) complexes and clay nanosheets. *Bull. Chem. Soc. Jpn.* 2020, 93, 194–199.
56. Onda, M.; Yoshihara, K.; Koyano, H.; Ariga, K.; Kunitake, T. Molecular recognition of nucleotides by the guanidinium unit at the surface of aqueous micelles and bilayers. A comparison of microscopic and macroscopic interfaces. *J. Am. Chem. Soc.* 1996, 118, 8524–8530.
57. Ariga, K. Molecular recognition at the air–water interface: Nanoarchitectonic design and physicochemical understanding. *Phys. Chem. Chem. Phys.* 2020, 22, 24856–24869.
58. Kurihara, K.; Ohto, K.; Tanaka, Y.; Aoyama, Y.; Kunitake, T. Molecular recognition of sugars by monolayers of resorcinol-dodecanal cyclotetramer. *J. Am. Chem. Soc.* 1991, 113, 444–450.
59. Kurihara, K.; Ohto, K.; Honda, Y.; Kunitake, T. Efficient, complementary binding of nucleic acid bases to diaminotriazine-functionalized monolayers on water. *J. Am. Chem. Soc.* 1991, 113, 5077–5079.
60. Ariga, K.; Kunitake, T. Molecular recognition at air–water and related interfaces: complementary hydrogen bonding and multisite interaction. *Acc. Chem. Res.* 1998, 31, 371–378.
61. Ariga, K.; Ito, H.; Hill, J.P.; Tsukube, H. Molecular recognition: From solution science to nano/materials technology. *Chem. Soc. Rev.* 2012, 41, 5800–5835.
62. Huo, Q.; Russell, K.C.; Leblanc, R.M. Effect of complementary hydrogen bonding additives in subphase on the structure and properties of the 2-amino-4,6-dioctadecylamino-1,3,5-triazine amphiphile at the air–water interface: Studies by ultraviolet-visible absorption spectroscopy and brewster angle microscopy. *Langmuir* 1998, 14, 2174–2186.
63. Neal, J.F.; Zhao, W.; Grooms, A.J.; Smeltzer, M.A.; Shook, B.M.; Flood, A.H.; Allen, H.C. Interfacial supramolecular structures of amphiphilic receptors drive aqueous phosphate recognition. *J. Am. Chem. Soc.* 2019, 141, 7876–7886.
64. Okuno, M.; Yamada, S.; Ohto, T.; Tada, H.; Nakanishi, W.; Ariga, K.; Ishibashi, T. Hydrogen bonds and molecular orientations of supramolecular structure between barbituric acid and melamine derivative at the air/water interface revealed by heterodyne-detected vibrational sum frequency generation spectroscopy. *J. Phys. Chem. Lett.* 2020, 11, 2422–2429.
65. Grooms, A.J.; Neal, J.F.; Ng, K.C.; Zhao, W.; Flood, A.H.; Allen, H.C. Thermodynamic signatures of the origin of anti-Hofmeister selectivity for phosphate at aqueous interfaces. *J. Phys. Chem. A* 2020, 124, 5621–5630.
66. Sakurai, M.; Tamagawa, H.; Inoue, Y.; Ariga, K.; Kunitake, T. Theoretical study of intermolecular interaction at the lipid–water interface. 1. Quantum chemical analysis using a reaction field theory. *J. Phys. Chem. B* 1997, 101, 4810–4816.
67. Tamagawa, H.; Sakurai, M.; Inoue, Y.; Ariga, K.; Kunitake, T. Theoretical study of intermolecular interaction at the lipid–water interface. 2. Analysis based on the Poisson–Boltzmann equation. *J. Phys. Chem. B* 1997, 101, 4817–4825.
68. Oishi, Y.; Torii, Y.; Kato, T.; Kuramori, M.; Suehiro, K.; Ariga, K.; Taguchi, K.; Kamino, A.; Koyano, A.H.; Kunitake, T. Molecular patterning of a guanidinium/orotate mixed monolayer through molecular recognition with flavin adenine dinucleotide. *Langmuir* 1997, 13, 519–524.
69. Ariga, K.; Mori, T.; Hill, J.P. Mechanical control of nanomaterials and nanosystems. *Adv. Mater.* 2012, 24, 158–176.
70. Ariga, K.; Yamauchi, Y.; Mori, T.; Hill, J.P. What can be done with the Langmuir-Blodgett method? Recent developments and its critical role in materials science. *Adv. Mater.* 2013, 25, 6477–6512.
71. Ariga, K. The evolution of molecular machines through interfacial nanoarchitectonics: From toys to tools. *Chem. Sci.* 2020, 11, 10594–10604.
72. Ariga, K.; Terasaka, Y.; Sakai, D.; Tsuji, H.; Kikuchi, J. Piezoluminescence based on molecular recognition by dynamic cavity array of steroid cyclophanes at the air–water interface. *J. Am. Chem. Soc.* 2000, 122, 7835–7836.
73. Ariga, K.; Nakanishi, T.; Terasaka, Y.; Tsuji, H.; Sakai, D.; Kikuchi, J. Piezoluminescence at the air–water interface through dynamic molecular recognition driven by lateral pressure application. *Langmuir* 2005, 21, 976–981.
74. Michinobu, T.; Shinoda, S.; Nakanishi, T.; Hill, J.P.; Fujii, K.; Player, T.N.; Tsukube, H.; Ariga, K. Mechanical control of enantioselectivity of amino acid recognition by cholesterol-armed cyclen monolayer at the air–water interface. *J. Am.*

75. Mori, T.; Okamoto, K.; Endo, H.; Hill, J.P.; Shinoda, S.; Matsukura, M.; Tsukube, H.; Suzuki, Y.; Kanekiyo, Y.; Ariga, K. Mechanical tuning of molecular recognition to discriminate the single-methyl-group difference between thymine and uracil. *J. Am. Chem. Soc.* 2010, 132, 12868–12870.
76. Sakakibara, K.; Joyce, L.A.; Mori, T.; Fujisawa, T.; Shabbir, S.H.; Hill, J.P.; Anslyn, E.V.; Ariga, K. A mechanically controlled indicator displacement assay. *Angew. Chem. Int. Ed.* 2012, 51, 9643–9646.
77. Mori, T.; Komatsu, H.; Sakamoto, N.; Suzuki, K.; Hill, J.P.; Matsumoto, M.; Sakai, H.; Ariga, K.; Nakanishi, W. Molecular rotors confined at an ordered 2D interface. *Phys. Chem. Chem. Phys.* 2018, 20, 3073–3078.
78. Mori, T.; Chin, H.; Kawashima, K.; Ngo, H.T.; Cho, N.-J.; Nakanishi, W.; Hill, J.P.; Ariga, K. Dynamic control of intramolecular rotation by tuning the surrounding two-dimensional matrix field. *ACS Nano* 2019, 13, 2410–2419.
79. Ishikawa, D.; Mori, T.; Yonamine, Y.; Nakanishi, W.; Cheung, D.J.; Hill, J.P.; Ariga, K. Mechanochemical tuning of the binaphthyl conformation at the air-water interface. *Angew. Chem. Int. Ed.* 2015, 54, 8988–8991.
80. Mori, T.; Ishikawa, D.; Yonamine, Y.; Fujii, Y.; Hill, J.P.; Ichinose, I.; Ariga, K.; Nakanishi, W. Mechanically induced opening-closing action of binaphthyl molecular pliers: Digital phase transition versus continuous conformational change. *ChemPhysChem* 2017, 18, 1470–1474.
81. Nakanishi, W.; Saito, S.; Sakamoto, N.; Kashiwagi, A.; Yamaguchi, S.; Sakai, H.; Ariga, K. Monitoring fluorescence response of amphiphilic flapping molecules in compressed monolayers at the air-water interface. *Chem. Asian J.* 2019, 14, 2869–2876.
82. Ishii, M.; Mori, T.; Nakanishi, W.; Hill, J.P.; Sakai, H.; Ariga, K. Helicity manipulation of a double-paddled binaphthyl in a two-dimensional matrix field at the air-water interface. *ACS Nano* 2020, 14, 13294–13303.
83. Adachi, J.; Mori, T.; Inoue, R.; Naito, M.; Le, N.H.-T.; Kawamorita, S.; Hill, J.P.; Naota, T.; Ariga, K. Emission control by molecular manipulation of double-paddled binuclear PtII complexes at the air-water interface. *Chem. Asian J.* 2020, 15, 406–414.
84. Mori, T.; Tanaka, H.; Dalui, A.; Mitoma, N.; Suzuki, K.; Matsumoto, M.; Aggarwal, N.; Patnaik, A.; Acharya, S.; Shrestha, L.K.; et al. Carbon nanosheets by morphology-retained carbonization of two-dimensional assembled anisotropic carbon nanorings. *Angew. Chem. Int. Ed.* 2018, 57, 9679–9683.
85. Krishnan, V.; Kasuya, Y.; Ji, Q.; Sathish, M.; Shrestha, L.K.; Ishihara, S.; Minami, K.; Morita, H.; Yamazaki, T.; Hanagata, N.; et al. Vortex-aligned fullerene nanowhiskers as a scaffold for orienting cell growth. *ACS Appl. Mater. Interfaces* 2015, 7, 15667–15673.
86. Watanabe, Y.; Sasabe, H.; Kido, J. Review of molecular engineering for horizontal molecular orientation in organic light-emitting devices. *Bull. Chem. Soc. Jpn.* 2019, 92, 716–728.
87. Yokoyama, D.; Sasabe, H.; Furukawa, Y.; Adachi, C.; Kido, J. Molecular stacking induced by intermolecular C–H...N hydrogen bonds leading to high carrier mobility in vacuum-deposited organic films. *Adv. Funct. Mater.* 2011, 21, 1375–1382.
88. Yokoyama, D. Molecular orientation in small-molecule organic light-emitting diodes. *J. Mater. Chem.* 2011, 21, 19187–19202.
89. Ariga, K. Don't forget Langmuir–Blodgett films 2020: Interfacial nanoarchitectonics with molecules, materials, and living objects. *Langmuir* 2020, 36, 7158–7180.
90. Yunoki, T.; Kimura, Y.; Fujimori, A. Maintenance properties of enzyme molecule stereostructure at high temperature by adsorption on organo-modified magnetic nanoparticle layer template. *Bull. Chem. Soc. Jpn.* 2019, 92, 1662–1671.
91. Rydzek, G.; Ji, Q.; Li, M.; Schaaf, P.; Hill, J.P.; Boulmedais, F.; Ariga, K. Electrochemical nanoarchitectonics and layer-by-layer assembly: From basics to future. *Nano Today* 2015, 10, 138–167.
92. Ariga, K.; Ahn, E.; Park, M.; Kim, B.S. Layer-by-layer assembly: Recent progress from layered assemblies to layered nanoarchitectonics. *Chem. Asian J.* 2019, 14, 2553–2566.
93. Zhang, X.; Xu, Y.; Zhang, X.; Wu, H.; Shen, J.; Chen, R.; Xiong, Y.; Li, J.; Guo, S. Progress on the layer-by-layer assembly of multilayered polymer composites: Strategy, structural control and applications. *Prog. Polym. Sci.* 2019, 89, 76–107.
94. Ito, M.; Yamashita, Y.; Tsuneda, Y.; Mori, T.; Takeya, J.; Watanabe, S.; Ariga, K. 100 °C-Langmuir-Blodgett method for fabricating highly oriented, ultrathin films of polymeric semiconductors. *ACS Appl. Mater. Interfaces* 2020, 12, 56522–56529.
95. Jackman, J.A.; Ferhan, A.R.; Cho, N.-J. Surface-based nanoplasmonic sensors for biointerfacial science applications. *Bull. Chem. Soc. Jpn.* 2019, 92, 1404–1412.

96. Ariga, K.; Ji, Q.; McShane, M.J.; Lvov, Y.M.; Vinu, A.; Hill, J.P. Inorganic nanoarchitectonics for biological applications. *Chem. Mater.* 2012, 24, 728–737.

---

Retrieved from <https://encyclopedia.pub/entry/history/show/24152>